BMC Cancer

RESEARCH

Open Access

Texasin, A main product from *Caragana Jubata (Pall.) Poir*, induces proliferation arrest and protective autophagy in lung adenocarcinoma

Liuzhao Cao[1,4†], Tiantian Li[2,4†], Xingxiang Xu[1,4], Mei Sun[3,4], Weiyun Teng[1,4*] and Miao Zhu[3,4*]

Abstract

Background Lung cancer, a leading cause of mortality worldwide, necessitates effective therapeutic strategies. *Caragana jubata*, a traditional Chinese medicinal plant, harbors Texasin, a potential anti-tumor agent. This study aimed to evaluate the anti-cancer effects of Texasin on lung cancer cells, while assessing its impact on normal lung cells.

Methods The study utilized cell lines H1299 and A549, alongside normal lung embryonic cells, to investigate Texasin's effects through Cell Counting Kit-8, Transwell, and wound healing assays. Transcriptome sequencing and analysis were performed to identify potential mechanisms. β-galactosidase activity and Retinoblastoma(RB) protein expression were assessed, and autophagy and apoptosis were explored through chloroquine co-treatment. Mice bearing H1299 cell-derived tumors were treated with Texasin. Tumor changes were assessed through in vivo imaging, and autophagy levels within the tumors were analyzed.

Results Texasin inhibited lung cancer cell proliferation, migration, and invasion without harming normal cells. It promoted cell senescence, arrested the cell cycle in G1 phase, and upregulated β-galactosidase and RB protein expression. Texasin induced protective autophagy, which could be converted to apoptosis by chloroquine co-treatment. Texasin inhibits the proliferation of lung adenocarcinoma cells in vivo, as evidenced by immunohistochemistry showing an increase in autophagy levels within the tumors.

Conclusions Texasin emerges as a promising non-cytotoxic anti-lung adenocarcinoma cancer compound, significantly inhibiting malignant phenotypes, highlighting its potential for lung adenocarcinoma cancer therapy.

Keywords Lung cancer, Tumor therapy, Traditional chinese medicine, Autophagy, Invasion and migration

†Liuzhao Cao and Tiantian Li contributed equally to this work.

*Correspondence:
Weiyun Teng
tengweiyun2023@163.com
Miao Zhu
realzhumiao@163.com

[1]Department of pulmonary and critical care medicine, Northern Jiangsu People's Hospital Affiliated to Yangzhou University, Jiangsu, People's Republic of China
[2]Department of Ultrasound, Northern Jiangsu People's Hospital Affiliated to Yangzhou University, Jiangsu, People's Republic of China
[3]Department of Hematology, Northern Jiangsu People's Hospital Affiliated to Yangzhou University, Jiangsu, People's Republic of China
[4]Northern Jiangsu People's Hospital, Jiangsu, People's Republic of China

Introduction

According to the American Cancer Society, it is estimated that there will be 2,001,140 new cancer cases and 611,720 cancer-related deaths in 2024. Among them, lung cancer accounts for approximately 20% of cancer-related deaths, posing a significant challenge to global public health [1]. Since 1991, more than 4 million deaths have been avoided due to advances in cancer screening methods, improved treatment plans, and scientific communication on the hazards of smoking. However, the high incidence of lung cancer is threatening this progress [2]. Lung cancer is histologically classified into two major categories: non-small cell lung cancer (NSCLC) and small cell lung cancer (SCLC), with NSCLC accounting for approximately 85% of all lung cancer cases [3]. Since most NSCLC patients do not have typical symptoms in the early stages, or even exhibit asymptomatic conditions, they are often diagnosed at advanced stages, making radical surgery inapplicable and leading to poor prognosis [4]. Cisplatin-based chemotherapy is the first-line treatment for patients with advanced lung cancer, but many patients cannot benefit from chemotherapy due to the significant toxicity and side effects of platinum-based drugs [5]. With the rapid development of molecular biology and in-depth research on the biological basis of lung cancer, molecular targeted drugs and immune checkpoint inhibitors for lung cancer are rapidly developing and have been applied in clinical practice [6]. Cytotoxic drugs like cisplatin lack specific markers to identify patient populations that may benefit from chemotherapy, which further limits the effectiveness of chemotherapy. Therefore, discovering and developing new, effective, and low-toxicity drugs for lung cancer treatment is the current major breakthrough.

Hanahan et al. defined malignant tumor as cells that have acquired a variety of capabilities, among which infinite proliferation is the most prominent feature of tumor [4]. Cellular senescence is a stable growth arrest caused by internal or external stress. The existence of cellular senescence or Hayflick limit is a natural barrier to the progression of precancerous lesions into tumors [7]. Therefore, targeting tumor senescence is gradually being considered as a tumor treatment strategy. 90% of lung cancer-related deaths are caused by metastasis of lung cancer, rather than primary tumors [8]. Metastasis of tumors is usually considered as a late-stage phenomenon, but due to its anatomical uniqueness, lung cancer often undergoes hematogenous metastasis in the early stage [9]. Once tumors detach from the primary site, they have three possible outcomes: apoptosis, dormancy, and development into new tumors. Most tumor cells die immediately after exudation, a very small number of cells enter a dormant state (in animal experiments, their proportion is 0.006%), and 0.01% of cells can develop into new tumors [10]. Preventing the invasion, metastasis, and proliferation of these cells is the key to treating lung cancer and prolonging the survival of patients.

KRAS mutation is one of the most prevalent oncogenic driver gene alterations in non-small cell lung cancer (NSCLC), accounting for approximately 25-30% of lung adenocarcinoma cases [11]. As a pivotal regulatory factor in the RAS/MAPK signaling pathway, mutations in KRAS protein, particularly hotspot mutations such as G12C and G12V, can lead to the sustained activation of downstream signaling, thereby promoting tumor cell proliferation, metastasis, and treatment resistance. However, the clinical management of KRAS-mutant lung cancer has long faced significant challenges: due to the lack of binding pockets for traditional small-molecule drugs on the KRAS protein surface and the high heterogeneity of mutant subtypes, this target was once considered "undruggable" by the academic community [12]. Although selective inhibitors targeting KRAS G12C mutations, such as sotorasib and adagrasib, have achieved breakthroughs through covalent binding to the "switch-II" pocket in recent years, their objective response rates (ORR) are only approximately 37-43%, with a median progression-free survival (mPFS) of 6.8 months, and effective targeted therapies remain lacking for mutant subtypes other than G12C [13, 14]. Furthermore, KRAS mutations often coexist with co-mutations such as TP53 and STK11, leading to significant variability in immune therapy responses, with ORR for monotherapy with PD-1/PD-L1 inhibitors being less than 20%. Overcoming KRAS mutation heterogeneity, developing broad-spectrum inhibitors, and optimizing combination therapy strategies remain core challenges in current research [13].

In China, the application of traditional Chinese medicine in treating tumors has a very long history and has been proven to have good curative effect and low toxicity [15, 16]. Texasin is extracted from *Caragana jubata (Pall.) Poir* (This name is the accepted name of a species in the genus *Caragana*, http://www.theplantlist.org/). *Caragana jubata* is a traditional Chinese medicine, which is called JinJiEr in China. According to the records in ancient Chinese medical books, JinJiEr is often used to treat cough and respiratory weakness caused by "XuLao" (which can be understood as weakness or fatigue), and to detoxify (cancer can be regarded as a kind of poison in traditional Chinese medicine). At present, JinJiEr is clinically used to treat lung cancer and other tumors. However, the effect of Texasin, the main active ingredient in JinJiEr, on lung cancer has not been reported yet.

Materials and methods

Cell culture

H1299 and A549 lung cancer cell lines were purchased from Zhong Qiao Xin Zhou Biotechnology (China).

Human embryonic lung cells MRC-5 were purchased from Procella Biotechnology (China). All cells were cultured strictly according to the instructions provided by the company and maintained in suitable media with 10% fetal bovine serum. H1299, A549, and MRC-5 were cultured in RPMI-1640, Ham's F-12 K, and MEM media, respectively. The cell culture incubator was set to 5% CO2, 37℃, and saturated humidity. The lung cancer cell lines were passaged every 3 days, and all experiments with MRC-5 cells were completed within 2 passages after purchase from the company.

Reagents and antibodies

Texasin was purchased from MedChemExpress(product code: HY-119822, CAS No. 897-46-1). Cell counting kit-8(product code: C0039), EdU cell proliferation kit with alexa fluor 488(product code: C0071L), Calcein/PI cell cytotoxicity assay kit(product code: C2015M), Senescence β-Galactosidase staining kit(product code: C0602), cell cycle and apoptosis analysis kit(product code: C1052), and BCA protein assay kit(P0009) were purchased from Beyotime Biotechnology. Antibody PCNA(product code: 13110 S), RB(product code: 9309 S), LC3B(product code: 3868 S), and B-actin(product code: 4970 S) were purchased from Cell Signaling Technology. Immunohistochemical antibody Ki67(GB111499), LC3B(GB13431), P62(GB11531) were purchased from Servicebio Technology. Gel preparation reagent kit(product code: BL522A) was purchased from Biosharp Life Sciences.

CCK-8 assay

The CCK-8 assay was used to detect the inhibitory effect of Texasin on lung cancer cells and provide a reference for selecting drug concentrations in subsequent experiments. Lung cancer cell lines were cultured in 96-well plates at an appropriate confluence and allowed to recover to their normal morphology. When the cell confluence reached approximately 60%, they were treated with Texasin. After 24–48 h of treatment, the drug-containing medium was aspirated (to prevent the drug from affecting absorbance), and pre-warmed medium containing 10% CCK-8 was added. The cells were then incubated for another hour. Subsequently, the absorbance values of each well were measured by a microplate reader. The absorbance values were normalized for analysis.

Cell proliferation assay

The synthesis of DNA requires thymine deoxyribonucleoside, and EdU (5-ethynyl-2'-deoxyuridine) is an analogue. When EdU is added during cell culture, it infiltrates into DNA and is labeled with Alexa Fluor 488 through click chemistry, enabling the detection of cells that are replicating DNA. In brief, after treating cells with Texasin for 48 h, EdU was added to the culture medium and the cells were further cultured for 2 h. Subsequently, the cells were fixed with 3.7% paraformaldehyde and permeabilized with 0.3% Triton X-100. The Click Additive Solution was prepared according to the instructions and incubated in the dark for 30 min. The cells were then washed three times with PBS containing 3% BSA, each time for 10 min. Subsequently, the cell nuclei were stained, and after staining, the cells were washed three more times, each time for 10 min. Finally, the fluorescence can be observed under a microscope.

Wound healing

The wound healing experiment was carried out by selecting cells in the logarithmic growth phase with healthy status to detect the migration ability of lung cancer cells. Cells were cultured in a 6-well plate at an appropriate density so that they can reach about 95% confluence overnight. Sterilized pipette tips (10ul) were used to scratch the cell surface perpendicularly, and the cells were washed three times with sterile PBS. Then, fresh medium containing drugs was added for further culture (the fetal bovine serum concentration in the medium is 2%). At specific time points (0 h, 24 h), the culture plate was taken out, and the healing of the scratch was observed and recorded by microscope photography. Image processing software (Image J) was used to analyze the scratch photos, measured the healing area of the scratch, and thereby evaluated the migration ability of the cells.

Transwell assay

The Transwell chamber was purchased from Corning(USA. Product number: 3422). For invasion experiments, matrix was applied to the upper chamber and incubated in an incubator to solidify. Lung cancer cells that had been treated with Texasin or control for 48 h were digested and counted, and adjusted to an appropriate density range, typically 1×10^6/ml. 200 μl of the cell suspension was added to the upper chamber, and the chamber containing the cells was placed in a 24-well plate with appropriate medium(non-serum-containing). The cells were further cultured for 24 h to allow for cell migration and invasion. Finally, the cells were fixed with paraformaldehyde and stained with 0.1% crystal violet solution. Gently wipe the cells in the upper chamber using a cotton swab. The number of cells that migrated through the membrane pores was observed and counted under a microscope.

Cytotoxicity assay

The Calcein/Propidium Iodide (PI) co-staining experiment was used to detect the toxic effect of Texasin on lung cancer cells. Calcein could only stain living cells, while PI could only stain dead cells with disrupted cell

membrane. Therefore, the combined use of Calcein and PI allowed for simultaneous fluorescent staining of live cells and dead cells with green and red fluorescence, respectively, for the detection of cell viability and cytotoxicity. Briefly, lung cancer cells treated with Texasin or control treatment for 48 h were stained with Calcein and PI in the dark for 30 min, and the staining results were observed by a fluorescence microscope. Finally, the number of living cells (green fluorescence) and dead cells (red fluorescence) were counted.

Protein immunoblotting

Cells were collected and lysed with RIPA, and the protein concentration of each sample was determined by the BCA assay. The protein samples were mixed with loading buffer in proportion and then heated at 95℃ for 5 min to ensure complete denaturation. 10% SDS-PAGE gels, including the separating gel and stacking gel, were prepared strictly according to the manufacturer's instructions. The protein samples were loaded into the SDS-PAGE gel wells, and vertical electrophoresis was carried out. After electrophoresis, the proteins on the gel were transferred onto a PVDF membrane by horizontal electrophoresis. The PVDF membrane was blocked with 5% skim milk to reduce nonspecific binding. The primary antibody incubation was performed overnight at 4℃ on a shaker (usually for 14 h), and the horseradish peroxidase-conjugated secondary antibody incubation was completed at room temperature (usually for 1 h). The PVDF membrane was washed three times with TBST for 10 min each to thoroughly remove unbound antibodies. A specific chemiluminescent substrate (luminol) was used to react with the horseradish peroxidase on the secondary antibody, producing luminescence. The image was captured using the Bio-Rad imaging system, and normalized analysis was performed on the gel image.

Detection of cell senescence

Logarithmically growing lung cancer cells were seeded in 6-well plates at a density of 2×10^5 cells per well. After the lung cancer cells were treated with or without Texasin for 48 h, they were washed once with PBS and fixed at room temperature for 15 min (the fixative was provided in the kit). After removing the fixative solution, the cells were washed with PBS three times. The staining working solution was strictly prepared according to the instructions and should be used immediately within 15 min after preparation. The staining step was carried out in a thermostat at 37 °C for 12 h (this step cannot be performed in a 5% CO_2 incubator). After the staining was completed, the cells were observed and photographed under an optical microscope.

Analysis of cell cycle distribution

Logarithmically growing lung cancer cells were seeded in 6-well plates at a density of 2×10^5 cells per well. Lung cancer cells were incubated for 48 h in either control medium or medium containing Texasin. The cells were then collected and fixed overnight at 4 °C using chilled 70% ethanol (with a minimum fixation time of 2 h), followed by RNase treatment. The propidium iodide (PI) staining working solution was prepared strictly according to the instructions. The staining step was performed for 30 min at 37 °C in a light-protected environment. The analysis of the cells was completed by a flow cytometer(BD FACS Verse), and the obtained data were analyzed by FlowJo software.

Immunofluorescence

Cells were cultured on surface-treated slides until they recovered their morphology (the thickness of the slides had to be less than 0.17 mm). After 48 h of control treatment or Texasin(80μM) treatment, the cells were fixed with 3.7% paraformaldehyde for 30 min and then permeabilized with a PBS solution containing 0.3% Triton X-100 for another 30 min. The blocking procedure for antigens was completed by TBS solution containing 5% BSA. The primary antibody was usually incubated overnight at 4 °C (typically around 14 h), while the secondary antibody was incubated at room temperature for 1 h in the dark. Finally, the cell nuclei were stained with DAPI solution for 15 min, and the cells were washed with PBS three times before imaging.

Cell infection

To detect the type of autophagy in cells, we constructed a lung cancer cell line expressing RFP-GFP-LC3B. The virus carrying the RFP-GFP-LC3B sequence was prepared and packaged by GeneChem(https://www.genechem.com.cn/). Cells were cultured in a well plate and when the confluence reached 30%, the serum-free medium containing the virus was added. After 16 h of infection, fresh serum-containing medium was replaced and the cells were further cultured for 24 h. The cells were then exposed to 2 μg/ml of puromycin for 48 h. When all cells could be observed with bright fluorescence, it was considered that the lung cancer cell line stably expressing the RFP-GFP-LC3B reporter system had been successfully constructed.

Apoptosis detection

Lung cancer cells were treated with the control or Texasin for 48 h. Floating cells and adherent cells in the culture medium were collected and washed with PBS solution for three times, followed by AnnV-FITC staining for 20 min. After adding PI solution, flow cytometry analysis could be performed.

Establishment of a xenograft animal model

A total of 18 five-week-old female BALB/c nude mice were purchased from the Comparative Medicine Research Institute of Yangzhou University (License No. SYXK[SU] 2014-0003) and acclimated for one week. H1299 cells were labeled with mCherry fluorescence and expanded. Each mouse was subcutaneously injected with 2×10^7tumor cells, which were suspended in 150 μL of PBS. Approximately 11 days after injection, when the tumors became externally prominent, the mice were randomly divided into three groups and treated with Texasin and DDP injections for one week. Mice in the Texasin group were intraperitoneal injected with texasin (10 mg/kg/day) every day. Mice in the DDP group were intraperitoneal injected with cisplatin (1 mg/kg/day) every other day. Euthanasia details, place the mouse in a CO_2 euthanasia device by gently positioning it in the induction chamber, where it will be exposed to a gradually increasing concentration of carbon dioxide (starting with pure CO_2 introduced at a rate of 30-50% per minute). After 5 min, confirm that the mouse heartbeat and respiration have completely ceased. All procedures have been pre-approved by the Institutional Animal Care and Use Committee of Yangzhou University (License No. SYXK[SU] 2022-0044).

Immunohistochemistry

The paraffin-embedded tissue samples were sectioned into 4-micron thick slices, deparaffinized in xylene, and rehydrated through a gradient of ethanol. Antigen retrieval was performed by heating the sections in pH 6.0 citrate buffer. Nonspecific binding and endogenous peroxidase activity were blocked using 3% hydrogen peroxide. The tissue sections were then incubated overnight at 4 °C with the primary antibody. Afterward, the sections were incubated with a biotin-conjugated secondary antibody, followed by horseradish peroxidase conjugation, and developed with 3,3′-diaminobenzidine tetrahydrochloride to visualize the labeled antigen.

Statistical analysis

All biologically related experiments in this study were repeated at least three times and statistically analyzed by SPSS 25.0. Differences between two groups were tested by t-tests, and differences between more than three groups were tested by one-way ANOVA. The differences were considered to be statistically significant when $^{*}P<0.05$, $^{**}P<0.01$, and $^{***}P<0.001$.

Results

Texasin inhibited the viability of lung cancer cells at non-toxic concentrations

The chemical structure of Texasin, as shown in Fig. 1A, is an isoflavone. By accessing the CCLE (Cancer Cell Line Encyclopedia) database, we selected the lung adenocarcinoma cell line A549, which harbors a KRAS mutation (G12S). Additionally, we included the lung adenocarcinoma H1299 cell line as a supplementary cell line, taking into account its status as a well-established model for drug screening. CCK-8 experiment preliminarily verified that Texasin had inhibitory effect on lung cancer cells, which was dose-dependent and time-dependent. Meanwhile, lung embryonic cells MRC-5 was insensitive to Texasin (Fig. 1B). By fitting the drug concentration and cell viability into the dose-response curve, the IC_{50} of Texasin on H1299 cell line were 123μM and 60.11μM (24 h and 48 h respectively), and the IC_{50} on A549 cell line were 233.4μM and 79.68μM (24 h and 48 h respectively). In addition, even high-concentration Texasin (80μM) did not show cytotoxicity to lung cancer cells (Fig. 1C), while the positive control drug DDP (20μM) led to a number of cell deaths. The killing rate of DDP (20 μm) against H1299 is about 88%, and the killing rate against A549 is about 76%. These results indicated that Texasin had a good inhibitory effect on the proliferation of lung adenocarcinoma cell with low cytotoxicity.

Texasin inhibited the proliferative ability of lung cancer

Since Texasin inhibited the proliferative ability of lung cancer cells without inducing cell death, We further conducted an EDU experiment on lung cancer cells treated with Texasin. After treating lung cancer cells with Texasin for 48 h, the percentage of dividing cells decreased significantly (Fig. 2A, B). The mean percentage of proliferating H1299 cells decreased from 47.0% in the control group to 32.3%, 7.3%, and 0.7%, respectively. The percentage of proliferating A549 cells decreased from 60.3% in the control group to 38.1%, 6.4%, and 0.3%, respectively. Meanwhile, the protein abundance of PCNA, a marker of lung cancer cell proliferation, was significantly reduced (Fig. 2C). These results indicate that Texasin inhibits the proliferative ability of lung cancer.

Texasin inhibited the migration and invasion of lung cancer

Lung cancer often undergoes distant metastasis by infiltrating blood vessels in the early stage. Then, we examined the effect of Texasin on the migration and invasion of lung cancer cells. After 24 h of Texasin treatment, the migration ability of lung cancer cells in the wound healing experiment was significantly reduced. In H1299 cells, the wound healing rate of the monolayer cells decreased from 85.2% in the control group to 51.3%, 23.4%, and 8.7% in the Texasin-treated groups, respectively. In A549 cells, the wound healing rate decreased from 88.8% in the control group to 59%, 26.4%, and 12%, respectively (Fig. 3A). In the Transwell experiment, the number of H1299 cells penetrating the 0.22-μm filter decreased from an average

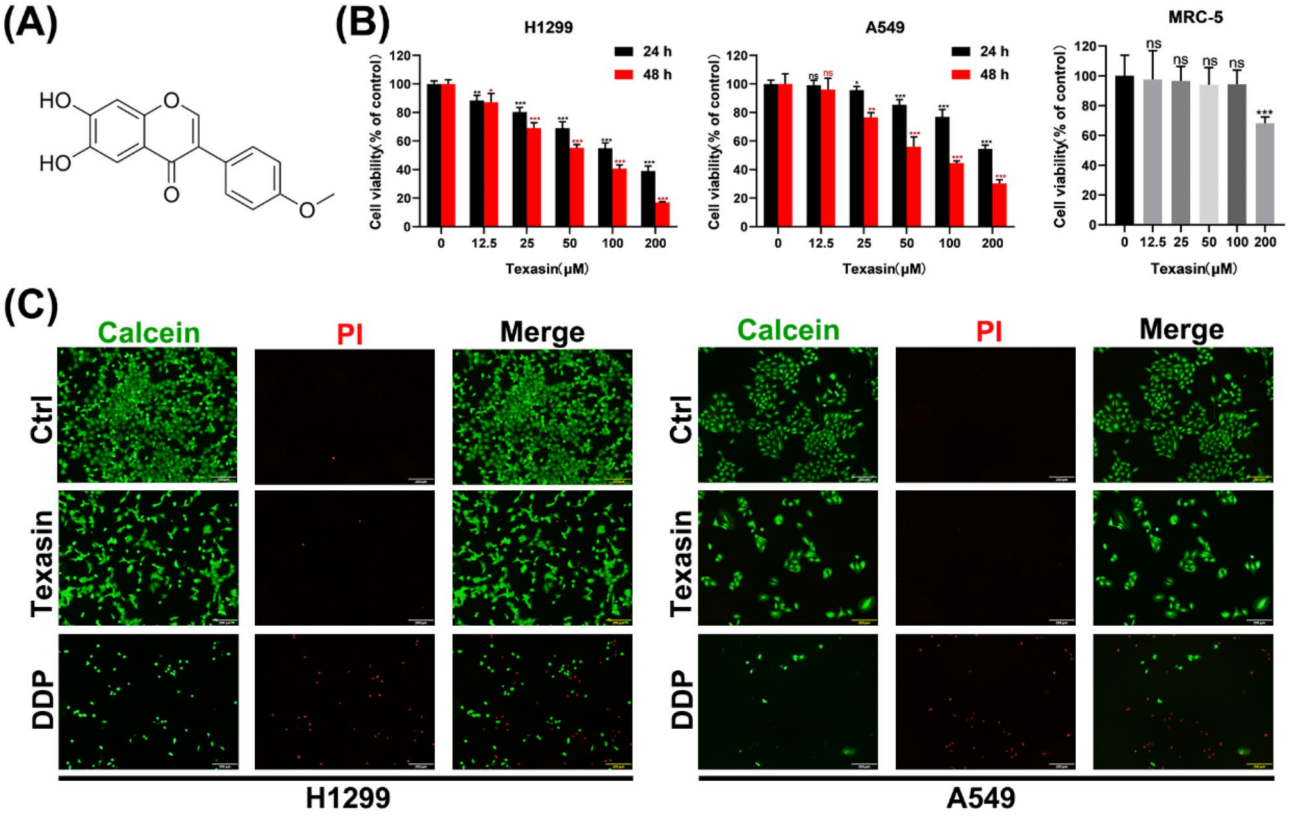

Fig. 1 Texasin inhibited the viability of lung cancer cells at non-toxic concentrations. (**A**) Chemical structure formula of Texasin. (**B**) CCK-8 assay of NSCLC after 24–48 h of Texasin treatment. The treatment time of Texasin on lung embryonic cells MRC-5 was 48 h.(**C**) The image of lung cancer cells stained with Calcein/Propidium Iodide after being treated with the specified concentrations of Texasin (80μM) and DDP (20μM) for 48 h. Scale Bar, 200 μm

of 311.4 in the control group to 155.3, 115.7, and 84.4 in the Texasin-treated groups, respectively. The number of A549 cells penetrating the filter decreased from an average of 422 in the control group to 287.3, 220.7, and 122.3 in the Texasin-treated groups, respectively (Fig. 3B). These results indicate that Texasin inhibits the migration and invasion of lung cancer.

Texasin inhibited lung cancer by promoting cell senescence and cell cycle arrest

To initially explore the specific mechanism of Texasin in inhibiting lung cancer, we performed transcriptome sequencing on A549 cells treated with or without Texasin, resulting in the identification of 2041 upregulated genes and 3333 downregulated genes (Fig. 4A). The KEGG analysis of these differentially expressed genes revealed that Texasin significantly regulates cell senescence and cell cycle (Fig. 4B). Further KEGG analysis of the significantly upregulated genes alone showed that they primarily function in regulating the Wnt and MAPK signaling pathways (Fig. 4C). Separately, the significantly downregulated genes were analyzed with KEGG, and they mainly regulate cell cycle and Neuroactive ligand-receptor interaction(Fig. 4D). To validate the reliability of these bioinformatics predictions, we conducted corresponding detection. After treatment with Texasin for 48 h, the level of β-galactosidase activity was significantly increased in lung cancer cells (Fig. 5A-B). Concurrently, Texasin significantly increased the expression of protein RB in cells (Fig. 5C), which is a tumor suppressor involved in cell senescence. After treatment with Texasin (80 μM) for 48 h, the G1 phase distribution in lung cancer cells was significantly increased, while the S phase distribution was significantly reduced(Fig. 5D-E). These results indicate that Texasin inhibits lung cancer by promoting cell senescence and cell cycle arrest.

Texasin induces protective autophagy in lung cancer cells

We found that a large amount of LC3B protein accumulated in H1299 and A549 cells after Texasin treatment(80μM), indicating the accumulation of autophagosomes (Fig. 6A-B). To elucidate the cause of autophagosome accumulation, we loaded the RFP-GFP-L3C reporter system into H1299 and A549 cells. Since the red fluorescent RFP can maintain its function under the acidic environment of lysosomes, while the green fluorescent GFP will be degraded, it can be used to determine whether autophagosomes fuse with lysosomes. As

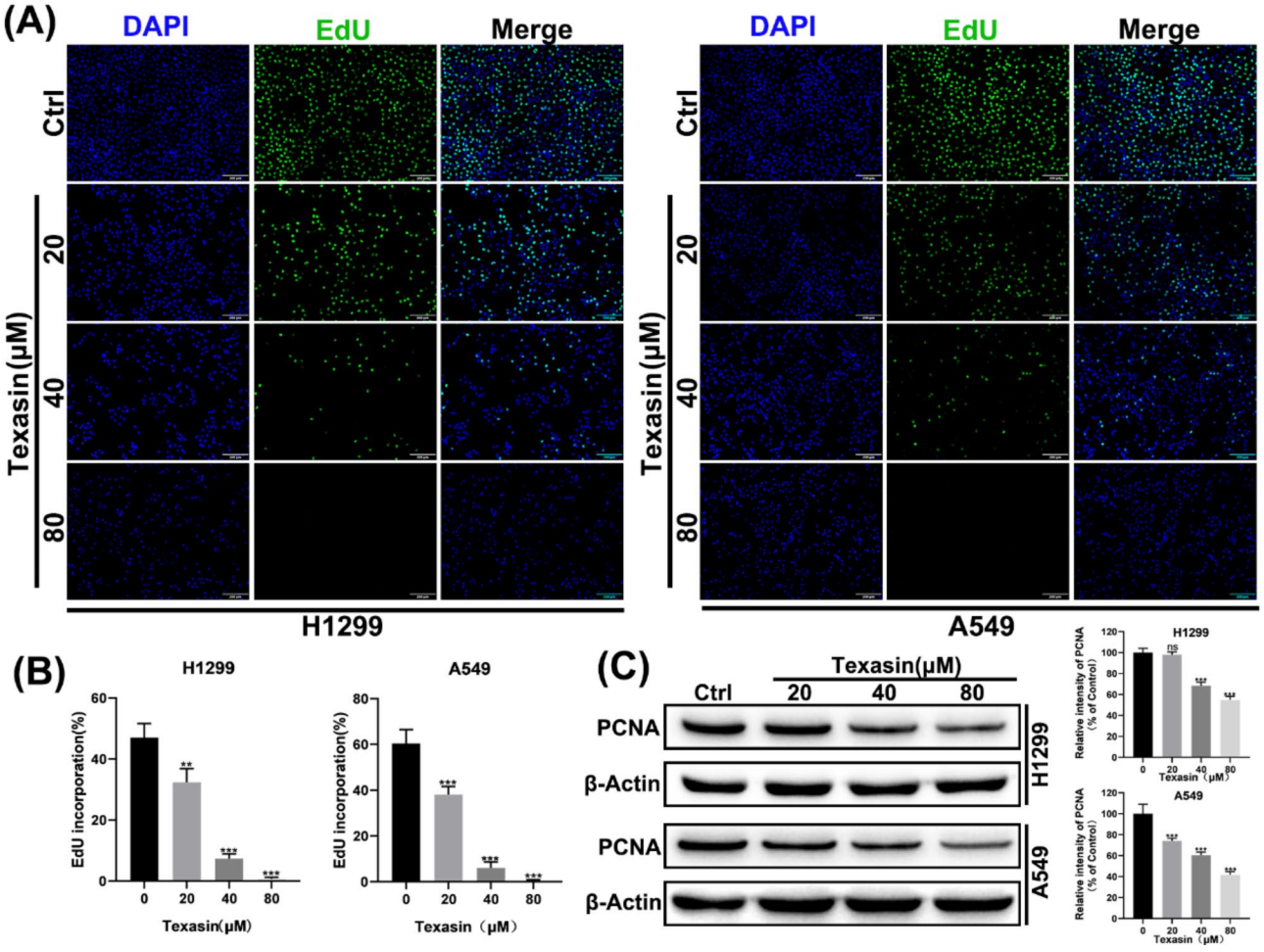

Fig. 2 Texasin inhibited the proliferative ability of lung cancer. (**A, B**) The EdU experiment was conducted on lung cancer cells after being treated with Texasin for 48 h. Scale Bar, 200 μm. Significant differences were observed between the groups. (**C**) The expression level of PCNA protein in lung cancer cells was analyzed by immunoblotting

shown in Fig. 6C-D, only a small number of red and green autophagic spots were observed in the control state, indicating a low level of autophagy. After 48 h of Texasin treatment(80μM), we observed a large number of red autophagic spots and a small number of green autophagic spots in the cells, indicating that most autophagosomes had fused with lysosomes and completed the autophagic flux. After treatment with the late-stage autophagy inhibitor chloroquine (CQ, 20μM) for 48 h, a large number of red and green autophagic spots appeared in the lung cancer cells, indicating that the autophagosomes could not fuse with lysosomes and the autophagic flux was blocked. The number of autophagic spots counted at this time could be considered as the basal autophagic flux of the cells within 48 h. When Texasin and CQ were combined to treat the cells for 48 h, a large number of autophagosomes were prevented from fusing with lysosomes, almost filling the entire cytoplasm. These autophagosomes could be considered as the autophagic flux that should have been produced by the cells exposed to Texasin(80μM) for 48 h.

The significance of autophagy to cells is usually dichotomous, helping cells adapt to environmental stress or causing autophagic cell death. To explore this issue, we used Texasin and CQ in combination. When autophagy was blocked by CQ, cell viability further decreased(Fig. 7A). Therefore, it can be concluded that autophagy induced by Texasin is an adaptive response of lung cancer cells to the drug. At the same time, we found that lung cancer cells underwent apoptosis when Texasin was combined with CQ(Fig. 7B-C). After 48 h of treatment with Texasin(80μM) alone, the percentage of apoptotic cells in H1299 cells was 4.82%, while it increased to 13.17% after 48 h of combined treatment with Texasin and CQ. After 48 h of treatment with Texasin alone, the percentage of apoptotic cells in A549 cells was 5.64%, while it increased to 21.26% after 48 h of combined treatment with Texasin and CQ. These results indicate that

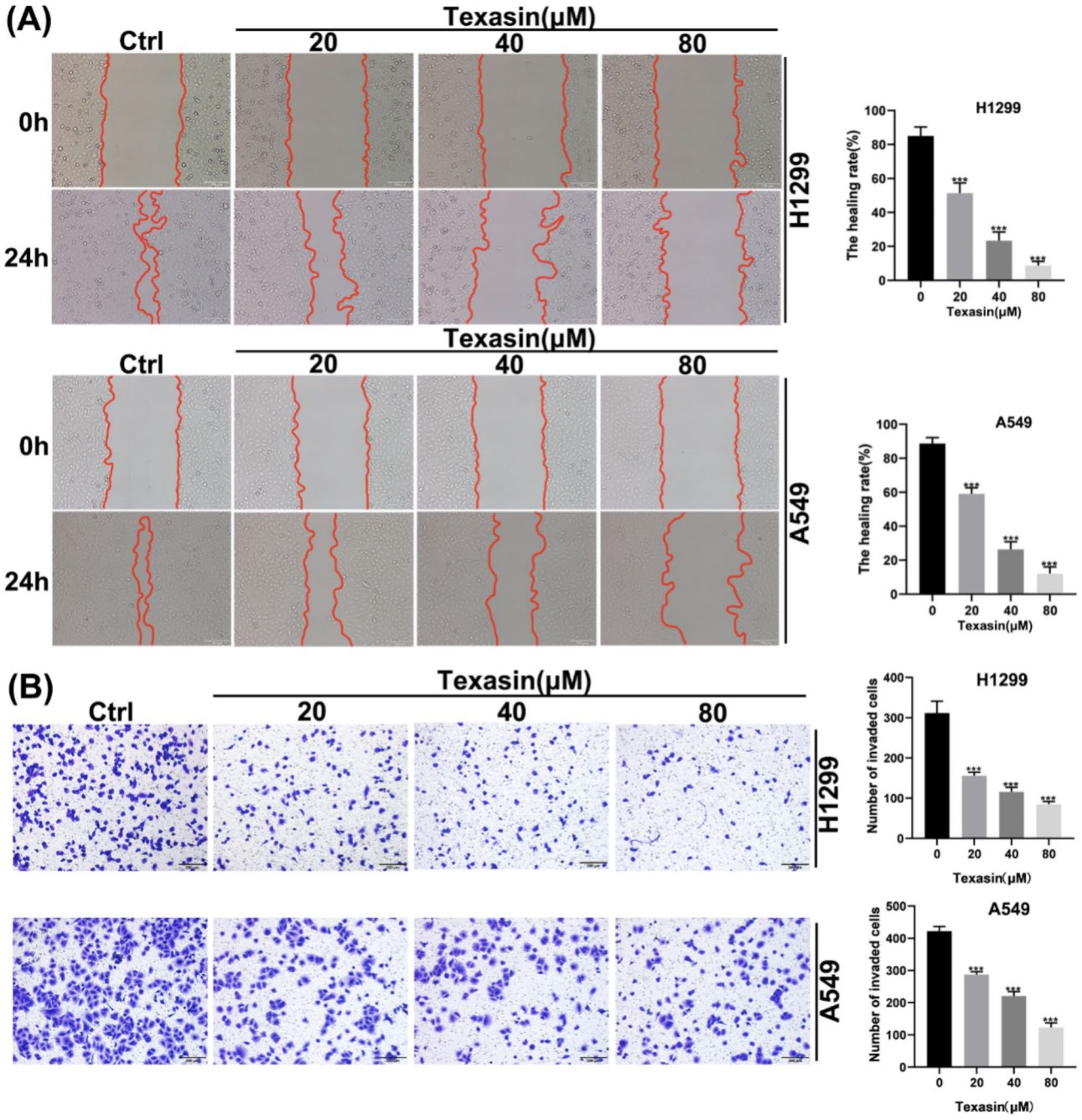

Fig. 3 Texasin inhibited the migration and invasion of lung cancer. (**A**) Wound healing of NSCLC cells before and after 24 h of treatment with different concentrations of Texasin. Scale bar, 200 μm. (**B**) Transwell assay of NSCLC cells after 24 h of treatment with different concentrations of Texasin. Scale bar, 200 μm

Texasin induces protective autophagy in lung cancer cells.

Texasin suppresses the process of lung cancer in vivo

To investigate the in vivo effects of Texasin on lung cancer, we established a tumor-bearing mouse model of lung cancer and performed small animal in vivo imaging. Compared to the positive control drug DDP, Texasin treatment resulted in reduced tumor volume and decreased tumor fluorescence intensity (Fig. 8A-B). Tumors were excised and weighed, showing that tumor weight significantly decreased in the Texasin-treated group compared to the CTRL group, with results demonstrating statistical significance (Fig. 8C). After intervention, there was no significant change in the body weight of the mice (Fig. 8D), but tumor volume was reduced

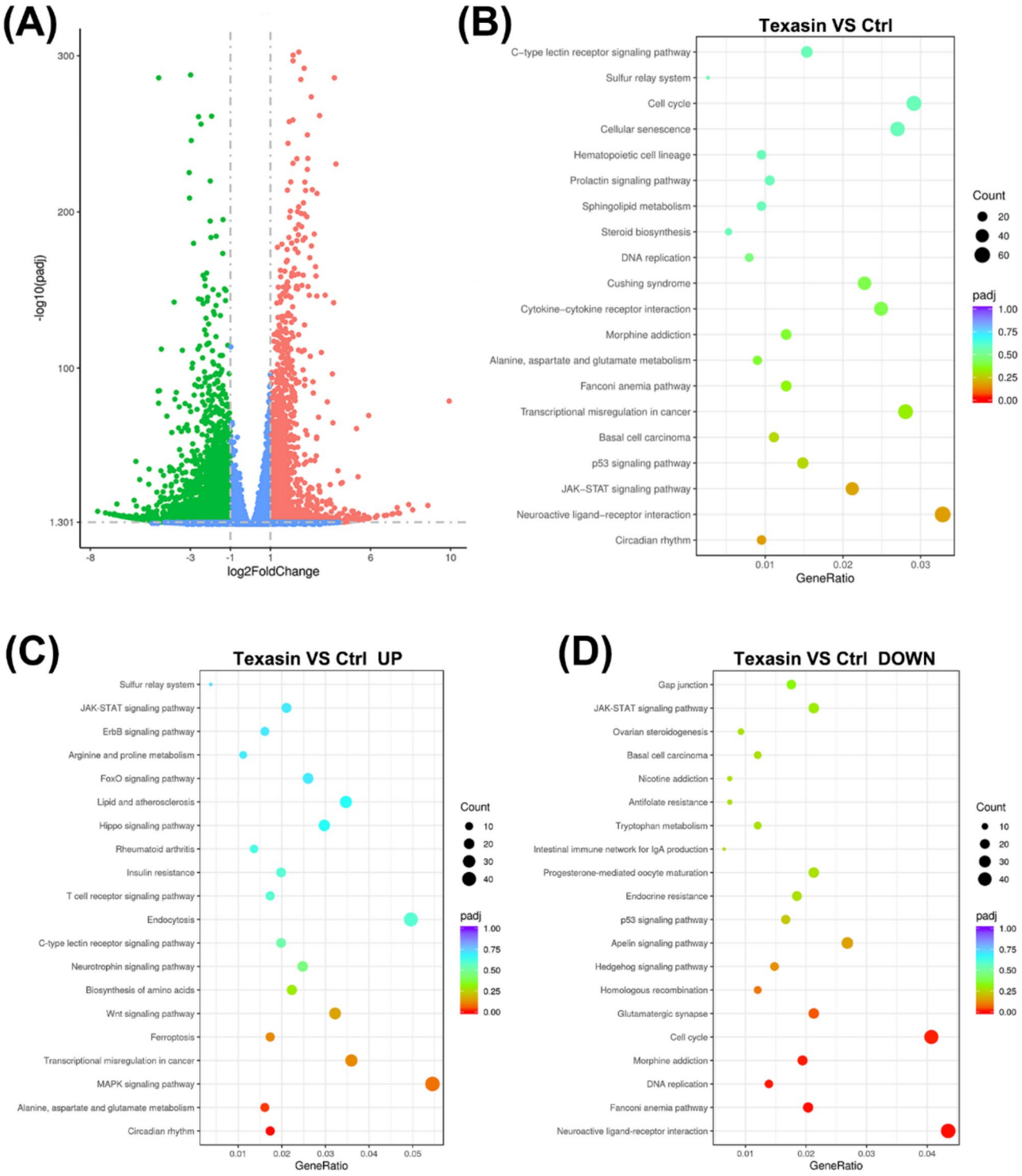

Fig. 4 Transcriptome Sequencing and KEGG Pathway Analysis. Volcano plot of differentially expressed genes in A549 cells treated with Texasin (80 μM) for 48 h compared to untreated cells. (**B-D**) KEGG pathway analysis of the differentially expressed genes

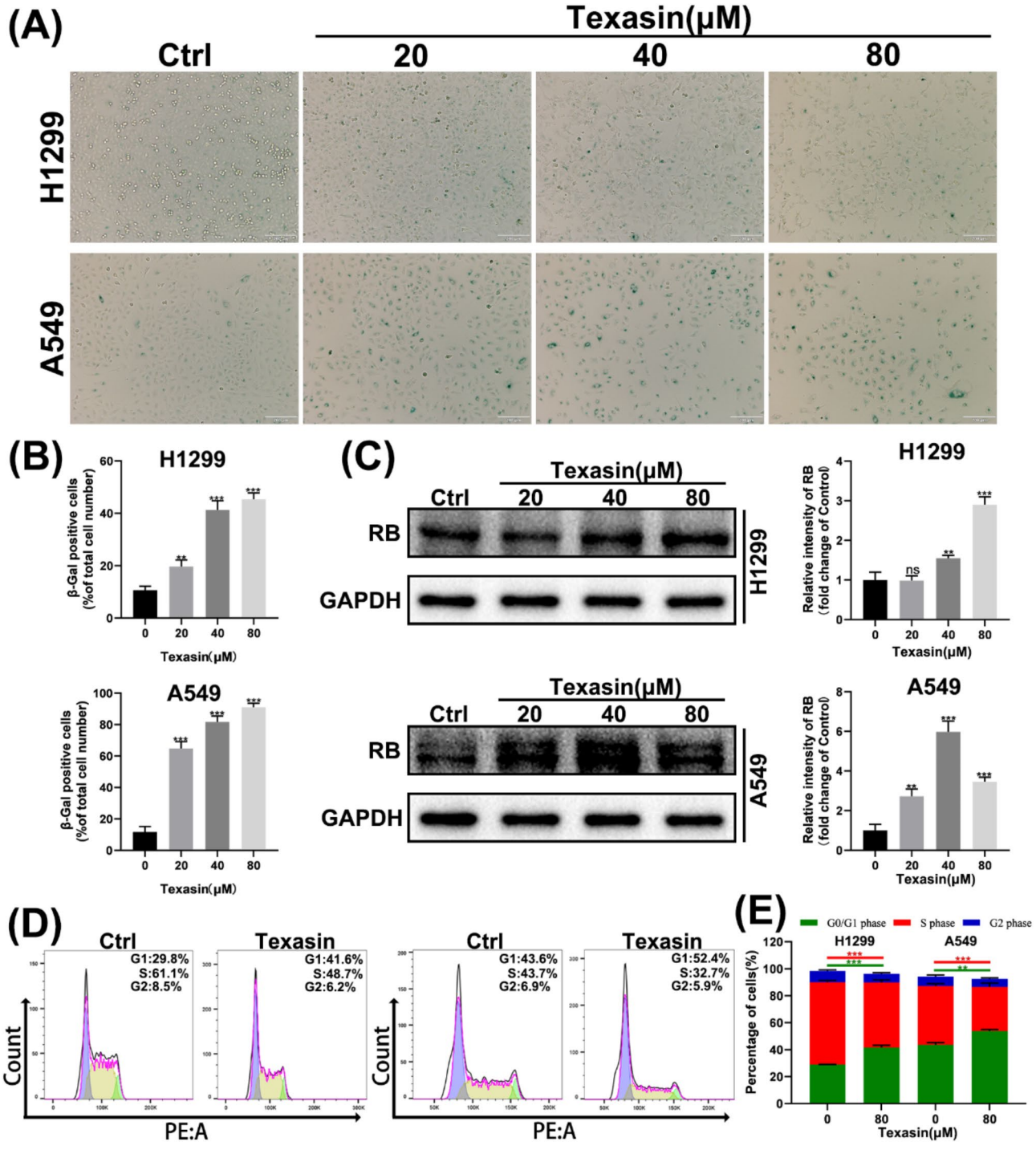

Fig. 5 Texasin promoted cell senescence and cell cycle arrest. (**A-B**)The image after β-galactosidase staining of lung cancer cells after 48 h of treatment with Texasin. Scale bar, 200 μm. (**C**) After 48 h of treatment with Texasin, the expression level of PCNA protein in lung cancer cells was analyzed by immunoblotting. (**D-E**)After 48 h of treatment with Texasin(80μM), flow cytometry was used to analyze the cell cycle distribution

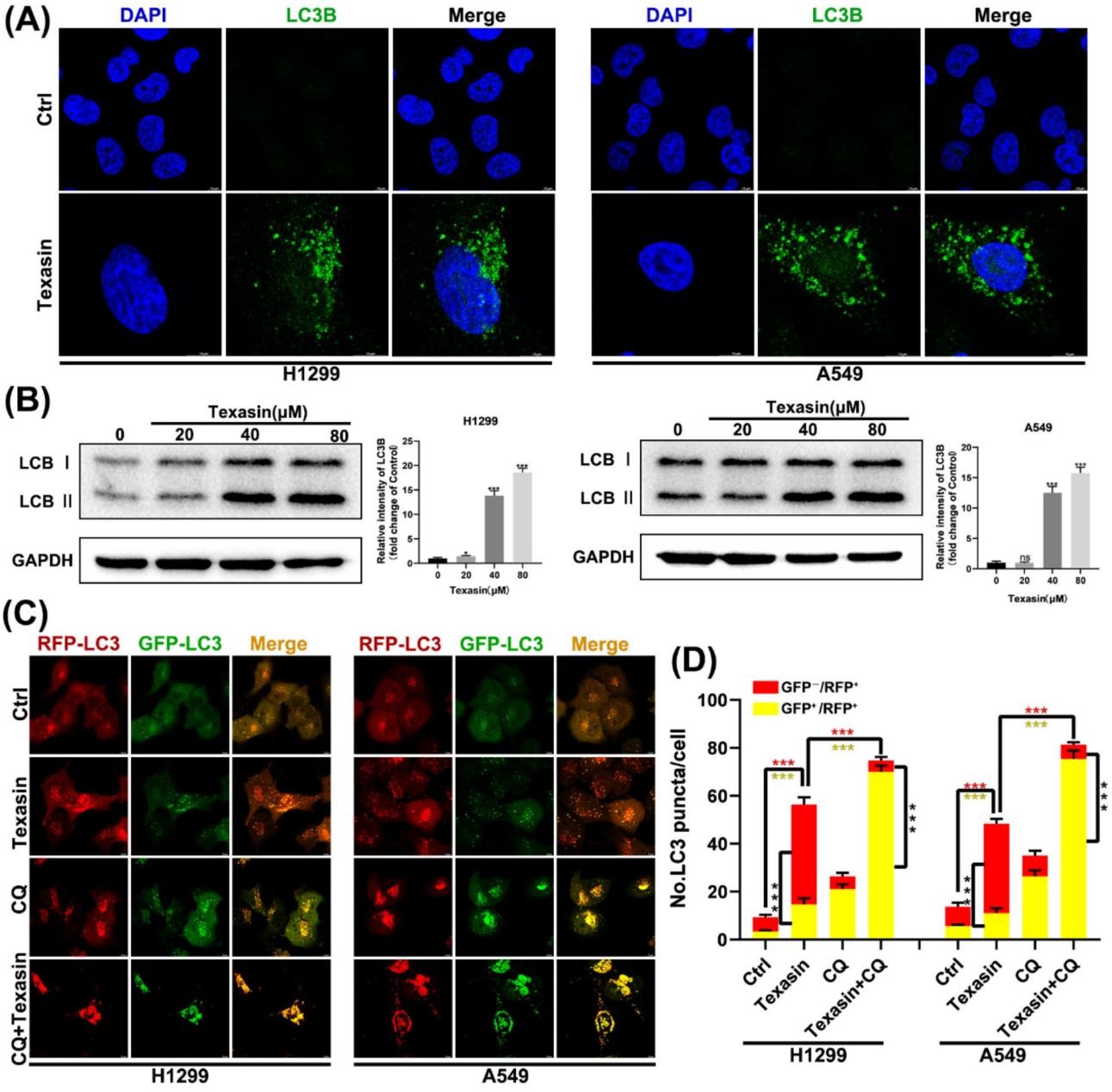

Fig. 6 Texasin increases the autophagic flux of lung cancer cells. (**A**) Representative images from the immunofluorescence experiment of lung cancer cells treated with control or Texasin(80μM) for 48 h. Scale bar, 10 μm. (**B**)Representative images from the immunoblot experiment after lung cancer cells were treated with the specified concentration of Texasin for 48 h. (**C-D**)Confocal laser scanning microscopy images of autophagic fluorescence within live cells after lung cancer cells were treated with Texasin(80μM), CQ(20μM), or a combination of both for 48 h. Scale bar, 10 μm

following Texasin treatment (Fig. 8E). In tumor immunohistochemical analysis, Ki67 expression decreased after Texasin treatment, with a more pronounced reduction observed in the positive control group. Autophagy-related markers showed an increase in LC3B and a decrease in P62, indicating that Texasin significantly impacts autophagy levels.

Discussion

Malignant tumor diseases, including lung cancer, have become a major challenge for global public health [1]. With the extensive and continuous development of biological research, especially the outstanding contributions of a large number of pharmaceutical talents, a variety of drugs approved for lung cancer treatment have emerged [17]. Currently, cisplatin-based therapeutic strategies are still the first-line regimen for lung cancer treatment. Although there are other treatment options available for

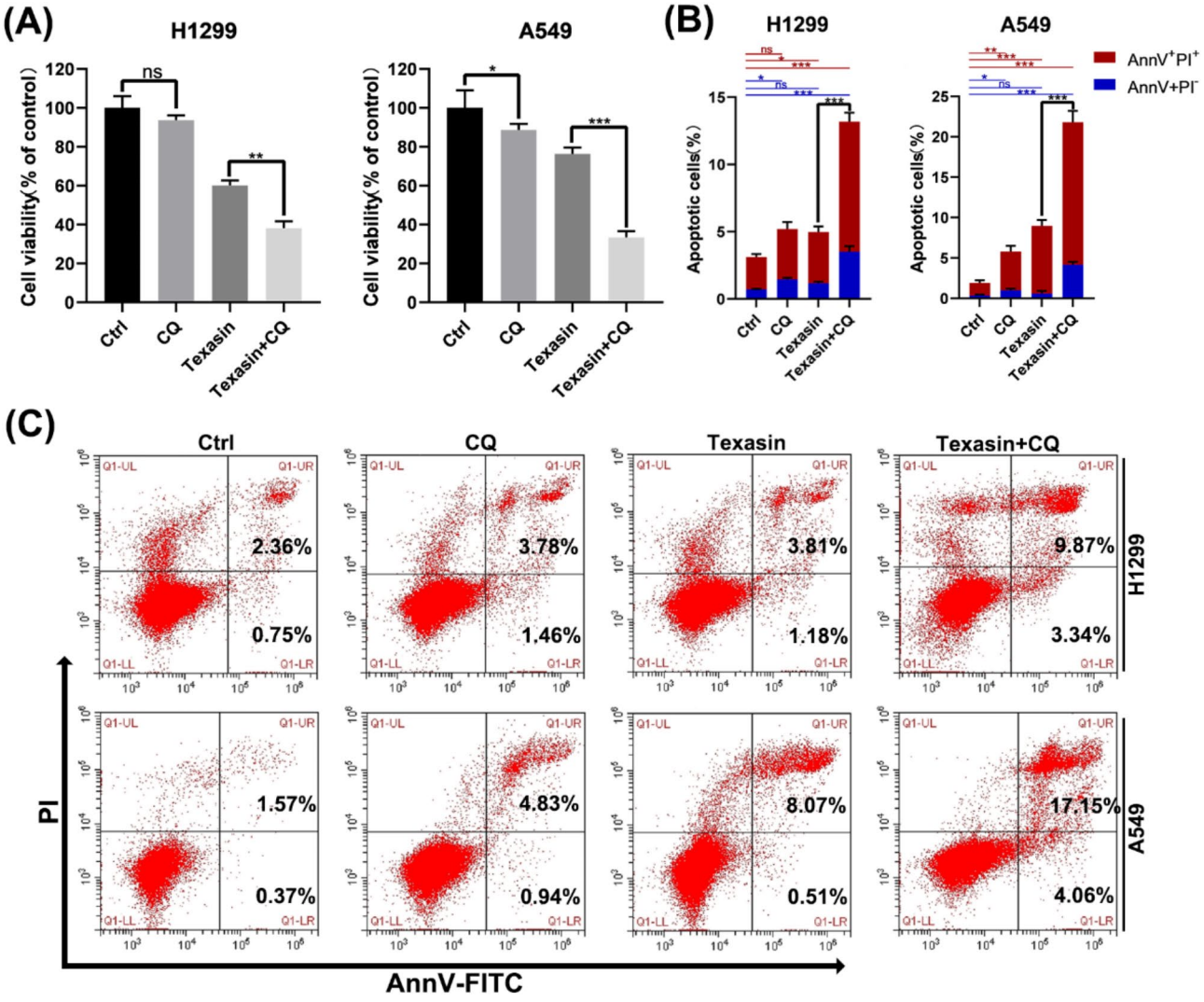

Fig. 7 Texasin induces protective autophagy in lung cancer cells. (**A**) The results of the CCK-8 experiment after lung cancer cells were treated with Texasin(80μM), CQ(20μM), or a combination of both for 24 h. (**B-C**) Flow cytometry analysis using double staining with AnnV-FLTC/PI was performed after lung cancer cells were treated with Texasin(80μM), CQ(20μM), or a combination of both for 48 h

patients who cannot tolerate chemotherapy, the significant side effects of tumor therapeutic drugs remain an inevitable problem [18]. In an ideal scenario, one would need to develop a drug that only inhibits the growth of tumor cells. In the CCK-8 experiment with a treatment time of 48 h, the IC_{50} values of Texasin on H1299 and A549 were 60.11μM and 79.68μM, respectively. For lung fibroblast MRC-5, even a concentration of 100μM did not show any inhibitory effect (Fig. 1). This indicates that the inhibitory effect of Texasin on lung cancer may be specific rather than indiscriminate cytotoxicity. The subsequent Calcein/Propidium Iodide double staining experiment also seemed to support this view, as Texasin did not induce tumor cell death. Therefore, Texasin may be a low-toxicity and effective drug for inhibiting lung cancer. It is noteworthy that Texasin failed to exhibit a significant inhibitory effect on two lung squamous cell carcinoma cell lines (H520 and H226, unpublished data). A549 represents a cell line harboring a KRAS mutation, which confers it with enhanced intrinsic drug resistance. Approximately 32% of patients with advanced lung adenocarcinoma possess KRAS mutations, directly leading to poor prognosis. Currently, there lacks an effective therapeutic strategy for these patients; however, Texasin still demonstrates a considerable inhibitory effect on A549 cells, thereby endowing this compound with broader application prospects.

Unlimited proliferation is the most significant characteristic of malignant tumors and the basis for cancer precursor lesions to become tumors [4]. In general, drug therapy can inhibit or kill most tumor cells, but there are always some cells that can gradually overcome this

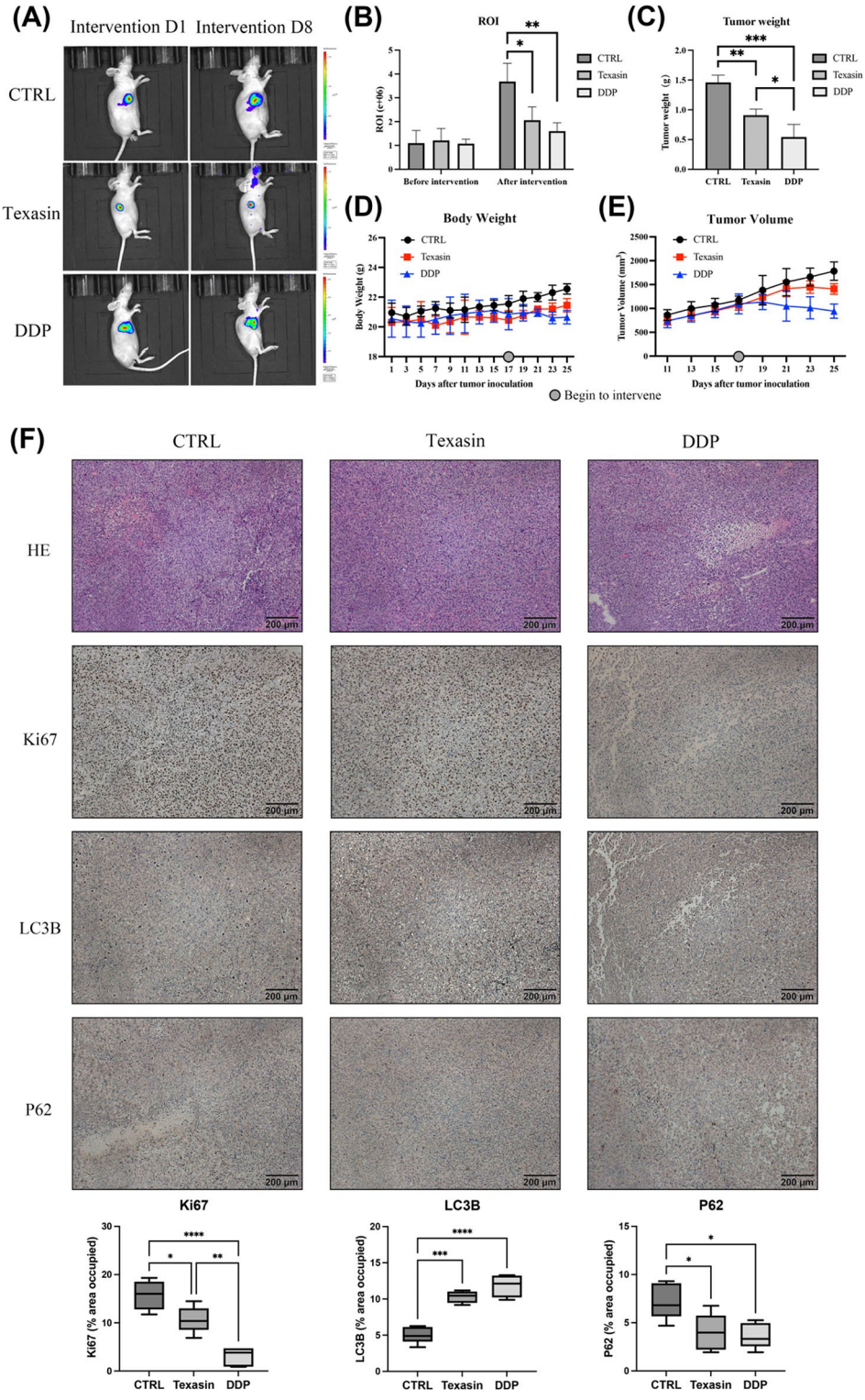

Fig. 8 Texasin suppresses the process of lung cancer in vivo. (**A**)Changes in tumor size in tumor-bearing mice with lung cancer after Texasin and PPD intervention. (**B**) In vivo imaging was used to detect changes in tumor fluorescence values in lung cancer-bearing mice before and after intervention. (**C-E**) Tumor weigh of tumor-bearing mice. Body weight, and tumor volume changes in each group of mice. (**F**) HE staining and immunohistochemical analysis of tumor tissues in three groups of mice

pressure. Some drug resistance is an inherent phenotype of tumors, such as drug efflux through ABC transporter family proteins [19]. More often, the drug-resistant phenotype of tumor cells is acquired, such as activating autophagy to adapt to stress or resisting drug effects through the activation of other non-target survival pathways, which is bypass resistance [20]. Therefore, drugs that can completely inhibit tumor growth are very rare. In our study, Texasin completely inhibited the proliferation of lung cancer cells. After 48 h of treatment with Texasin(80μM), no EdU infiltration was observed in lung cancer cells(Fig. 2). The in vivo results indicate that Texasin treatment inhibits tumor cell proliferation, with modest reduction in tumor growth when used alone. We believe the potential value of Texasin lies in its role as a cytostatic agent, best utilized in combination with other cytotoxic drugs(Fig. 8). Meanwhile, the cell proliferation marker PCNA was also reduced to a very low level. For lung cancer, 90% of deaths are caused by distant metastasis rather than the primary tumor [21]. In people's long-standing understanding of tumor diseases, distant metastasis seems to be a unique manifestation of the late stage of cancer. However, due to the unique structure of lung tissue, lung cancer can metastasize through lymphatic vessels and blood vessels in stage II [22]. Therefore, preventing distant metastasis of tumors is of great significance for those patients with unresectable lung cancer. This study demonstrates that Texasin can significantly inhibit the migration and invasion abilities of lung cancer cells (Figs. 3 and 4). By reducing the serum content in the culture medium, we have basically eliminated the influence of cell proliferation on invasion and migration experiments, and Texasin(80μM) significantly reduced the invasive phenotype of lung cancer cells. These results indicate that the inhibition of lung cancer proliferation by Texasin is thorough and it serves as an effective inhibitor of invasion and migration.

Autophagy is an evolutionarily conserved cytoplasmic process where cells are able to "eat" parts of themselves [23]. Initially, autophagy was often observed in dying cells and was thought of as a form of cell death. However, as research progressed, it was discovered that when cells face adverse factors such as environmental stress and nutrient deprivation, autophagy can engulf parts of itself to eliminate damaged organelles and release essential amino acids back into the cytoplasm to supply substrates required for synthetic processes [24]. Currently, numerous studies have reported that autophagy aids tumor cells in drug resistance and prevents cell death. Meanwhile, research has also shown that the application of autophagy inhibitors like chloroquine can help patients better fight tumor diseases [25]. This study found that Texasin increased the autophagic flux in lung cancer cells, and inhibiting this autophagic process promoted cell apoptosis (Figs. 6, 7 and 8). Ki67 was significantly reduced in both the Texasin and DDP groups compared to the control, indicating the anti-proliferative effects of both treatments. However, the reduction in Ki67 expression was more pronounced in the DDP group, suggesting that DDP have a stronger inhibitory effect on tumor cell proliferation than Texasin. LC3B showed significantly higher expression in the Texasin and DDP groups compared to the control, indicating enhanced autophagy induction. P62 was reduced in both the Texasin and DDP groups compared to the control, further supporting autophagy activation(Figs. 8). These findings suggest that while both Texasin and DDP exhibit anti-tumor effects, their mechanisms of action may differ in strength and pathway preference. Texasin appears to induce autophagy more robustly. It is not difficult to infer that the increased autophagy flux induced by Texasin represents a protective autophagy through which lung cancer cells may eliminate damaged organelles and accelerate the recycling of internal nutrients. Therefore, these results indicate that the activation of autophagy induced by Texasin is a protective response of lung cancer cells to the drug.

Senescence is a response of cells to various pressures or signals, with the most important feature being that cells no longer enter the cell cycle and maintain a stable cell state [26]. Previously, studies on senescence almost never focused on tumor cells, but current research shows that tumor cells can also enter senescence. On one hand, the malignant phenotype of senescent tumor cells will degenerate, and on the other hand, they will attract host immune cells to eliminate them. Currently, inducing and utilizing the senescence of tumor cells is being considered as a new tumor treatment method [27]. This study found that Texasin significantly increased the activity of β-galactosidase (Fig. 6), which is the earliest and most widely used marker of cell senescence. Meanwhile, Texasin significantly upregulated the expression of protein RB. Generally, the inhibition of various CDKs (such as p21 and p16) on the cell cycle can lead to the excessive activation of RB, which will cause cell senescence and cycle arrest. Existing results show that senescence will lead to cells exiting the cell cycle, but lung cancer cells treated with Texasin did not completely exit the cell cycle. Instead, they were blocked at various stages, with an increased proportion of G1 phase and a reduced proportion of S phase. Therefore, we believe that Texasin inhibiting the proliferation of lung cancer is not completely achieved by promoting senescence, and there should be other important pathways. Meanwhile, the target of Texasin is still unclear, and the next step of research will reveal the biological target of Texasin, which will also help explain the specific reasons for the stagnation of lung cancer cell proliferation.

Conclusions

This study demonstrates that Texasin has significant anti-lung cancer activity with lower toxicity to normal lung embryonic cells. Texasin is able to induce complete growth arrest in non-small cell lung cancer and inhibit its invasive phenotype. The possible mechanism is the promotion of cellular senescence and cell cycle arrest.

Abbreviations

NSCLC	Non-small cell lung cancer
SCLC	Small cell lung cancer
RB	Retinoblastoma
CCK-8	Cell counting kit-8
PCNA	Proliferating Cell Nuclear Antigen
LC3B	Microtubule-associated protein 1 light chain 3 beta
EdU	5-ethynyl-2′-deoxyuridine
PI	Propidium Iodide
BCA	Bicinchoninic acid
PBS	Phosphate Buffered Saline
PVDF	Polyvinylidene Difluoride
TBST	Tris-Buffered Saline with Tween-20
TBS	Tris-Buffered Saline
DAPI	4′,6-Diamidino-2′-phenylindole
RFP-GFP	Red Fluorescent Protein-Green Fluorescent Protein
DDP	Cisplatin
CQ	Chloroquine
KEGG	Kyoto Encyclopedia of Genes and Genomes

Supplementary Information

The online version contains supplementary material available at https://doi.org/10.1186/s12885-025-13933-3.

Supplementary Material 1

Supplementary Material 2

Acknowledgements

The authors would like to express their gratitude to the supporting colleagues at the Key Laboratory of Syndrome Differentiation and Treatment of Gastric Cancer of the State Administration of Traditional Chinese Medicine.

Author contributions

Acquisition: Liuzhao Cao; Miao Zhu. Methodology: Tiantian Li; Xingxiang Xu. Resources Software: Weiyun Teng; Mei Sun. Writing—review and editing: Liuzhao Cao.

Funding

Research Fund project of Norther Jiangsu People's Hospital (SBHL22004, SBQN22010); Postgraduate Research & Practice Innovation Program of Jiangsu Province (SJCK22_1813); National Natural Science Foundation of China(82405499).

Data availability

Data is provided within the manuscript or supplementary information files.

Declarations

Competing interests

The authors declare no competing interests.

Received: 18 November 2024 / Accepted: 13 March 2025
Published online: 20 March 2025

References

1. Siegel RL, Giaquinto AN, Jemal A. Cancer statistics. CA Cancer J Clin. 2024;74(1):12–49. https://doi.org/10.3322/caac.21820.
2. Siegel RL, Miller KD, Wagle NS, Jemal A. Cancer statistics. CA Cancer J Clin. 2023;73(1):17–48. https://doi.org/10.3322/caac.21763.
3. Rudin CM, Brambilla E, Faivre-Finn C, Sage J. Small-cell lung cancer. Nat Rev Dis Primers. 2021;7(1):3. https://doi.org/10.1038/s41572-020-00235-0.
4. Hanahan D. Hallmarks of Cancer: New Dimensions. Cancer Discov, 2022,12(1):31-46.10.1158/2159–8290.CD-21-1059.
5. Camidge DR, Doebele RC, Kerr KM. Comparing and contrasting predictive biomarkers for immunotherapy and targeted therapy of NSCLC. Nat Rev Clin Oncol, 2019,16(6):341-355.10.1038/s41571-019-0173-9.
6. Sung H, Ferlay J, Siegel RL, Laversanne M, Soerjomataram I, Jemal A et al. Global Cancer Statistics 2020: GLOBOCAN Estimates of Incidence and Mortality Worldwide for 36 Cancers in 185 Countries. CA Cancer J Clin, 2021,71(3):209-249.10.3322/caac.21660.
7. D'Ambrosio M, Gil J. Reshaping of the tumor microenvironment by cellular senescence: an opportunity for senotherapies. Dev Cell. 2023;58(12):1007–21. https://doi.org/10.1016/j.devcel.2023.05.010.
8. Wang Y, Narasimamurthy R, Qu M, Shi N, Guo H, Xue Y, et al. Circadian regulation of cancer stem cells and the tumor microenvironment during metastasis. Nat Cancer. 2024;5(4):546–56. https://doi.org/10.1038/s43018-024-00776-3.
9. Wang X, Bai H, Zhang J, Wang Z, Duan J, Cai H, et al. Genetic intratumor heterogeneity remodels the immune microenvironment and induces immune evasion in brain metastasis of lung cancer. J Thorac Oncol. 2024;19(2):252–72. https://doi.org/10.1016/j.jtho.2023.09.276.
10. Perlikos F, Harrington KJ, Syrigos KN. Key molecular mechanisms in lung cancer invasion and metastasis: a comprehensive review. Crit Rev Oncol Hematol. 2013;87(1):1–11.
11. Wang M, Herbst RS, Boshoff C. Toward personalized treatment approaches for non-small-cell lung cancer. Nat Med. 2021;27:1345–56.
12. Ostrem JM, Shokat KM. Direct small-molecule inhibitors of KRAS: from structural insights to mechanism-based design. Nat Rev Drug Discov. 2016;15:771–85.
13. Canon J, Rex K, Saiki AY, Mohr C, Cooke K, Bagal D, Gaida K, Holt T, Knutson CG, Koppada N, et al. The clinical KRAS(G12C) inhibitor AMG 510 drives anti-tumour immunity. Nature. 2019;575:217–23.
14. Hallin J, Engstrom LD, Hargis L, Calinisan A, Aranda R, Briere DM, Sudhakar N, Bowcut V, Baer BR, Ballard JA, et al. The KRAS(G12C) inhibitor MRTX849 provides insight toward therapeutic susceptibility of KRAS-Mutant cancers in mouse models and patients. Cancer Discov. 2020;10:54–71.
15. Li Z, Feiyue Z, Gaofeng L. Traditional Chinese medicine and lung cancer–From theory to practic. Biomed Pharmacother, 2021,137:111381.10.1016/j.critrevonc.2012.12.007.
16. Huang Z, Huang Q, Ji L, Wang Y, Qi X, Liu L et al. Epigenetic regulation of active Chinese herbal components for cancer prevention and treatment: A follow-up review. Pharmacol Res, 2016,114:1-12.10.1016/j.phrs.2016.09.023.
17. Alduais Y, Zhang H, Fan F, Chen J, Chen B. Non-small cell lung cancer (NSCLC): A review of risk factors, diagnosis, and treatment. Med (Baltim). 2023;102(8):e32899. https://doi.org/10.1097/MD.0000000000032899.
18. Li Y, Yan B, He S. Advances and challenges in the treatment of lung cancer. Biomed Pharmacother. 2023;169:115891. https://doi.org/10.1016/j.biopha.2023.115891.
19. Youmbi LM, Makong YSD, Mbaveng AT, Tankeo SB, Fotso GW, Ndjakou BL, et al. Cytotoxicity of the methanol extracts and compounds of Brucea antidysenterica (Simaroubaceae) towards multifactorial drug-resistant human cancer cell lines. BMC Complement Med Ther. 2023;23(1):48. https://doi.org/10.1186/s12906-023-03877-1.
20. Lim ZF, Ma PC. Emerging insights of tumor heterogeneity and drug resistance mechanisms in lung cancer targeted therapy. J Hematol Oncol. 2019;12(1):134. https://doi.org/10.1186/s13045-019-0818-2.
21. Xie S, Wu Z, Qi Y, Wu B, Zhu X. The metastasizing mechanisms of lung cancer: recent advances and therapeutic challenges. Biomed Pharmacother. 2021;138:111450. https://doi.org/10.1016/j.biopha.2021.111450.
22. Martínez-Ruiz C, Black JRM, Puttick C, Hill MS, Demeulemeester J, Larose Cadieux E, et al. Genomic-transcriptomic evolution in lung cancer and metastasis. Nature. 2023;616(7957):543–52. https://doi.org/10.1038/s41586-023-05706-4.
23. Liu S, Yao S, Yang H, Liu S, Wang Y, Autophagy. Regulator of cell death. Cell Death Dis, 2023,14(10):648.10.1038/s41419-023-06154-8.
24. Mizushima N, Levine B. Autophagy in human diseases. N Engl J Med. 2020;383(16):1564–76. https://doi.org/10.1056/NEJMra2022774.

25. Moulana MS, Haiaty S, Bazmani A, Shabkhizan R, Moslehian MS, Sadeghsoltani F, et al. Tumoricidal properties of thymoquinone on human colorectal adenocarcinoma cells via the modulation of autophagy. BMC Complement Med Ther. 2024;24(1):132. https://doi.org/10.1186/s12906-024-04432-2.
26. Jochems F, Thijssen B, De Conti G, Jansen R, Pogacar Z, Groot K, et al. The cancer senescopedia: A delineation of cancer cell senescence. Cell Rep. 2021;36(4):109441. https://doi.org/10.1016/j.celrep.2021.109441.
27. Wang L, Lankhorst L, Bernards R. Exploiting senescence for the treatment of cancer. Nat Rev Cancer. 2022;22(6):340–55. https://doi.org/10.1038/s41568-022-00450-9.

Publisher's note